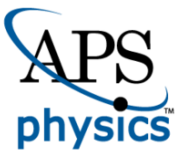

Topological Charge Pumping in Excitonic Insulators

Zhiyuan Sun and Andrew J. Millis

Phys. Rev. Lett. **126**, 027601 — Published 12 January 2021

DOI: 10.1103/PhysRevLett.126.027601

Topological charge pumping in excitonic insulators

Zhiyuan Sun[1] and Andrew J. Millis[1,2]

[1]*Department of Physics, Columbia University, 538 West 120th Street, New York, New York 10027*
[2]*Center for Computational Quantum Physics, Flatiron Institute, 162 5th Avenue, New York, NY 10010*

(Dated: November 12, 2020)

We show that in excitonic insulators with s-wave electron-hole pairing, an applied electric field (either pulsed or static) can induce a p-wave component to the order parameter, and further drive it to rotate in the $s+ip$ plane, realizing a Thouless charge pump. In one dimension, each cycle of rotation pumps exactly two electrons across the sample. Higher dimensional systems can be viewed as a stack of one dimensional chains in momentum space in which each chain crossing the fermi surface contributes a channel of charge pumping. Physics beyond the adiabatic limit, including in particular dissipative effects is discussed.

Controlling many-body systems, and in particular using appropriately applied external fields to 'steer' order parameters of symmetry broken phases, has emerged as a central theme in current physics [1–8]. The excitonic insulator (EI) is state of matter first proposed in the 1960s [9–12] with an order parameter defined as a condensate of bound electron hole pairs that activates a hybridization between two otherwise (in the simplest case) decoupled bands and opens a gap in the electronic spectrum. Several candidate materials including electron-hole bilayers [13–15], Ta_2NiSe_5 [16–21], $1T$-$TiSe_2$ [22–25] and monolayer WTe_2 [26] are objects of current intensive study; recent work [15, 27–31] has pointed out their possible topological aspects. While the early theories of EI considered a one component order parameter, typically of inversion symmetric s-wave type, realistic interactions also allow for electron-hole pairing in sub-dominant channels including p-wave (inversion-odd) ones. In equilibrium, the s-wave ground state is favored, with the potential for p-wave order revealed by its fluctuations accompanied by dipole moment oscillations: the 'Bardasis-Schrieffer' collective mode [32].

In this paper we show that applied electric fields can steer the order parameter to rotate in the space of s and p symmetry components, as shown in Fig. 1(a), leading to a realization of the 'Thouless charge pump' [33–36], providing quantized charge transport across an insulating sample.

The minimal model of an EI involves two electron bands shown in Fig. 1(b): a valence band with energy $\xi_{v,k}$ that disperses downwards from a high symmetry point (taken to have zero momentum) and a conduction band ($\xi_{c,k}$) that disperses upwards. For simplicity we assume that their energies are equal and opposite ($\xi_c = -\xi_v = \xi$). Relaxing this assumption does not change our results in an essential way. Defining the overlap $G = 2\xi_{v,0}$, we distinguish the 'BCS' case $G > 0$ where the two bands cross at a fermi wavevector k_F with fermi velocity v_F as shown by the dashed lines, leading to electron and hole pockets, and the 'BEC' case where $G < 0$ and the bands do not cross. Excitonic order corresponds to the spontaneous formation of a hybridization between the two bands due to the electron-electron interaction V, leading to an order parameter $\Delta(k) = \sum_{k'} V_{k-k'} \langle \psi^\dagger_{c,k'} \psi_{v,k'} \rangle + c.c.$ where $\psi_{c/v,k}$ is the electron annihilation operator at momentum k of the conduction/valence band and V_q is the Fourier transform of the density-density interaction potential $V(r)$. The s-wave order parameter $\Delta_s(k)$ is invariant under crystal symmetry operations while p-wave order parameters are odd under inversion: $\Delta_p(k) = -\Delta_p(-k)$, and often transform as a multi-dimensional representation of the crystal symmetry group. For simplicity we neglect the k-dependence of Δ_s, and define $\Delta_p(k) = \Delta_p f_k$ where the pairing function f_k carries the momentum dependence and satisfies $\max(|f_{k_F}|) = 1$. We focus on the p_x pairing channel which is induced by the x-direction electric fields we consider here. While the qualitative conclusions hold generically for all spatial dimensions, we will indicate the dimensionality if a specific d-dimensional system is discussed where the momentum k means a d-dimensional vector.

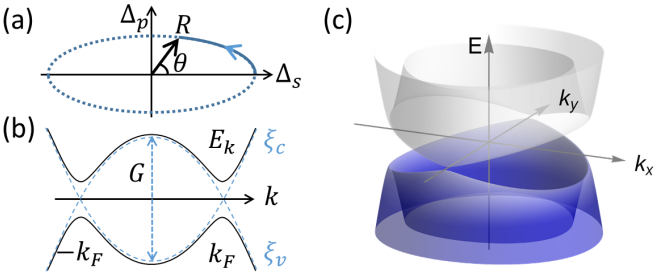

FIG. 1. (a) The $s+ip$ plane for the excitonic order parameter, with electric field-driven evolution shown as dashed line. (b) The quasiparticle dispersion in a one dimensional EI (solid lines) along with bands in metallic phase (dashed lines). (c) The band dispersion of a two dimensional EI with an $s+ip$ order parameter and $\Delta_s \ll \Delta_p$.

Writing the partition function Z as a path integral over fermion fields $\psi = (\psi_c, \psi_v)$, performing a Hubbard-Stratonovich transformation of the interaction term in the excitonic pairing channel and subsuming the intraband interaction into ξ one obtains the action (see [37] Sec. I)

$$S = \int d\tau dr \left\{ \psi^\dagger (\partial_\tau + H_m) \psi + \frac{1}{g_s} |\Delta_s|^2 + \frac{1}{g_p} |\Delta_p|^2 \right\} \quad (1)$$

as an integral over space-time (r, τ) and the partition function is $Z = \int D[\bar{\psi}, \psi] D[\bar{\Delta}, \Delta] e^{-S}$. For physically reasonable

interactions such as the screened Coulomb interaction, the s-wave pairing interaction g_s is typically the strongest while g_p is the leading subdominant one. We may write the mean field Hamiltonian as $\int dr\psi^\dagger H_m\psi = \sum_k \psi_k^\dagger H_m^k \psi_k$ with

$$H_m^k[\Delta_s,\Delta_p] = \xi_k\sigma_3 + \Delta_s\sigma_1 + \Delta_p f_k\sigma_2 \tag{2}$$

where σ_i are the Pauli matrices acting in the c/v band space. The vector potential A enters Eq. (2) through the minimal coupling $k \to k - A$ required by local gauge invariance (electric field is $E = -\partial_t A$) and we set electron charge e, speed of light and the Planck constant $\hbar$ to be one. Interband dipolar couplings could also occur [6, 38] but do not affect our results. Since the global phase is not important, we choose the s-wave order parameter to be real. As we will show, the system develops an electrical polarization as a p-wave component $\pi/2$ out of phase with the equilibrium Δ_s is introduced. Due to an emergent 'particle hole' symmetry in the BCS weak coupling case defined as $|\Delta_s|, |\Delta_p| \ll G$ which we focus on, applied electric fields create Δ_p primarily in this channel (see Sec. VI A of [37] for a rigorous proof), so we write p-wave pairing in the σ_2 channel [32]. The quasiparticle spectrum is $E_k = \pm\sqrt{\xi_k^2 + \Delta_s^2 + \Delta_p^2 f_k^2}$. As shown by Fig. 1(c), the spectrum will have gapless points (nodes) at $(k_x, k_y) = (0, \pm k_F)$ in the pure p-wave state ($\Delta_s = 0$) in two dimension (2D).

Charge pump—Spatially uniform changes in $\Delta_{s,p}$ produce uniform currents $J = \langle \sum_k \partial_k H_m^k \rangle$ (see [37] Sec. II), whose time integral from the initial $(\Delta_s, \Delta_p) = (\Delta, 0)$ to the final point then gives the pumped charge P (difference of polarization between the final state and the initial state). In a one dimensional (1D) system, P has a geometrical meaning [35, 39] in the limit of slow order parameter dynamics. It is the flux of the Berry curvature 2-form B through the 2D surface S spanned by the occupied 1D crystal momentum k and the time varying trajectory of $\Delta_{s,p}$, or alternatively by the line integral of the Berry connection $\mathscr{A}_\mu = i\langle\psi|\partial_\mu|\psi\rangle$ around its boundary:

$$P = \frac{1}{2\pi}\int_S dS\cdot B = \frac{1}{2\pi}\oint dl\cdot\mathscr{A} \tag{3}$$

where $\mu = (k, \Delta_s, \Delta_p)$ (see Fig. 2).

The Berry curvature B from the valence band of Eq. (2) is sourced by monopoles at the points $\xi_k = \Delta_s = \Delta_p = 0$, i.e., the points $(k, \Delta_s, \Delta_p) = (\pm k_F, 0, 0)$ each of which has monopole charge 1. If the order parameter evolution completes a full cycle on the $s+ip$ plane, S becomes the surface of the 2-torus shown in Fig. 2(a) and the net charge pumped is the total flux from the enclosed monopoles which is an integer $N = 2$, the Chern number of the process. This quantized change in the polarization is known as the Thouless pump [33], a topological phenomenon immune to disorder. Note that the monopoles exist only for the 'BCS' ($G > 0$, band inversion) case where the excitons strongly overlap such that charge can jump between them. In the 'BEC' case

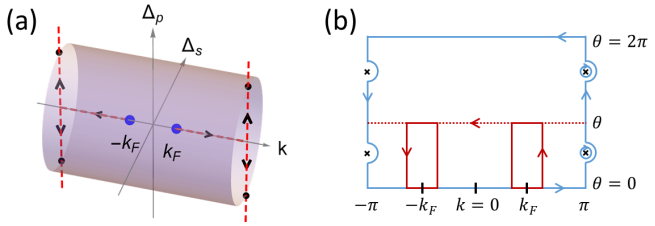

FIG. 2. (a) The surface S in the (k, Δ_s, Δ_p) space used to calculate the flux of the Berry curvature for a 1D EI for which the order parameter evolution completes a full cycle in the $s+ip$ plane. The left and right ends of the cylinder are identified so that S is a 2-torus. Blue dots are Berry curvature monopoles and red dashed lines are 'Dirac strings' with direction shown by black arrows. (b) The surface of the torus shown in (a) parametrized by k and θ with $k = \pm\pi$ and $\theta = 0, 2\pi$ identified. The blue contours yield the charge pumped during a full cycle. The red rectangles are used to compute the flux for a partial cycle in the BCS limit.

$\xi_k \neq 0$ for all k and there are no monopoles enclosed in S (see [37] Sec. II C).

To compute the polarization for the case the order parameter does not complete a full cycle, we use the line integral approach. For notational simplicity, we suppress the subscripts 'k' without causing ambiguities. An explicit expression for the valence band wave function from (2) at (k, Δ_s, Δ_p) is

$$|\psi\rangle = (-v^*, u^*) = \frac{1}{\sqrt{2E(E-\xi)}}\left(\xi - E, \Delta^*\right) \tag{4}$$

where $\Delta = \Delta_s + i\Delta_p f_k \equiv |\Delta| e^{i\phi}$ and $|u|^2(|v^2|) = \frac{1}{2}\left(1 \pm \frac{\xi}{E}\right)$. The Berry connection $\mathscr{A}_\mu = |u|^2\partial_\mu\phi$ has singularities associated with the Dirac strings, the intersections of which with S (marked by crosses in Fig. 2(b)) must be correctly treated in the evaluation of the line integral. Noting that $|u|^2 \to 0$ when $\xi \ll -|\Delta|$ and $|u|^2 \to 1$ when $\xi \gg |\Delta|$, we see that in the weak coupling BCS limit the contour can be collapsed to the red rectangles in Fig. 2(b). Parameterizing S using k and the angle θ defined by $\Delta_s + i\Delta_p = Re^{i\theta}$ in Fig. 1(a), one observes that the polarization of an state on the $s+ip$ plane depends only on the angle θ. Specifically, we found

$$P = \theta/\pi \tag{5}$$

for a 1D EI (see [37] Sec. II). This may be understood by noting that the low energy physics around $\pm k_F$ is of two massive Dirac models, each of which realizes a Goldstone-Wilczek [40] mechanism of charge pumping.

Higher dimensional systems can be viewed as 1D chains along x direction stacked in momentum space. For a 2D circular fermi surface one finds

$$P(\theta) = \begin{cases} \frac{k_F}{2\pi}\tan\frac{\theta}{2} & (0 < \theta < \pi/2) \\ \frac{k_F}{2\pi}\left(2 - \cot\frac{\theta}{2}\right) & (\pi/2 < \theta < \pi) \\ \frac{k_F}{\pi} + P(\theta - \pi) & (\pi < \theta < 2\pi) \end{cases}. \tag{6}$$

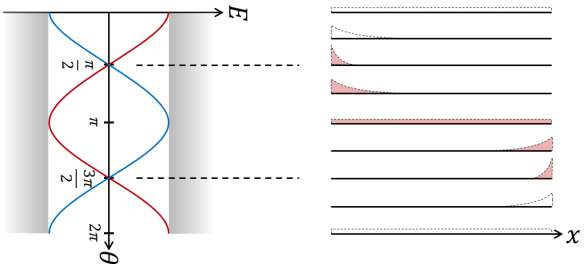

FIG. 3. Left is the evolution of the edge state energies as a function of θ. Right is the spatial profile of one of the two edge states (labeled by red line on the left) neglecting its quick oscillating detail. Being filled means the state is occupied. The blue edge state is not shown but is the mirror image of the red one.

A full cycle pumps exactly two electrons along each 1D momentum chain that crosses the fermi surface, giving

$$P_{1D} = 2, \quad P_{2D} = \frac{2k_F}{\pi}, \quad P_{3D} = \frac{k_F^2}{2\pi} \tag{7}$$

for 1D, 2D and three dimensional (3D) isotropic systems respectively.

Although the charge pump is a bulk property carried by all valence band electrons, it is also revealed by the evolution of edge states as Δ_s and Δ_p are varied, as shown in Fig. 3 for a 1D wire connected with reservoirs. In the BCS limit, with open boundary conditions $\psi(0) = \psi(L) = 0$, there are two edge states

$$\psi_\pm = \frac{1}{C_\pm}(1, \pm 1)\sin(k_F x)e^{\mp x\Delta_p/v_F}, \quad E = \pm\Delta_s \tag{8}$$

where $C_\pm$ is a normalization constant. We suppose $\Delta_s + i\Delta_p = Re^{i\theta}$ and follow the evolution of ψ_+ as θ is varied (see Fig.3). At $\theta = 0$ the state is delocalized and unoccupied with energy R. As θ is increased the state becomes localized near $x = 0$ and decreases in energy. When θ passes through $\pi/2$, the state becomes maximally localized and becomes occupied by an electron from the left reservoir since its energy crosses the chemical potential. As θ further increases the state becomes delocalized and then localized at the right edge, delivering its electron to the right reservoir when θ crosses $3\pi/2$. Considering the ψ_- state during the same cycle, two electrons in total are pumped. In higher dimensions, each 1D k_x chain crossing the fermi surface has a similar edge state evolution (see [37] Sec. III).

Dynamics—The coupled dynamics of electrons and the order parameters in the presence of an applied electric field is described by the action Eq. (1). To understand the qualitative dynamics, we use a low energy effective Ginzburg-Landau Lagrangian

$$L(\Delta_s, \Delta_p; E) = F - K + L_{\text{drive}} \tag{9}$$

for fields Δ_s, Δ_p obtained by integrating out the Fermions (see [37] Sec. IV). The dynamics is given by the standard

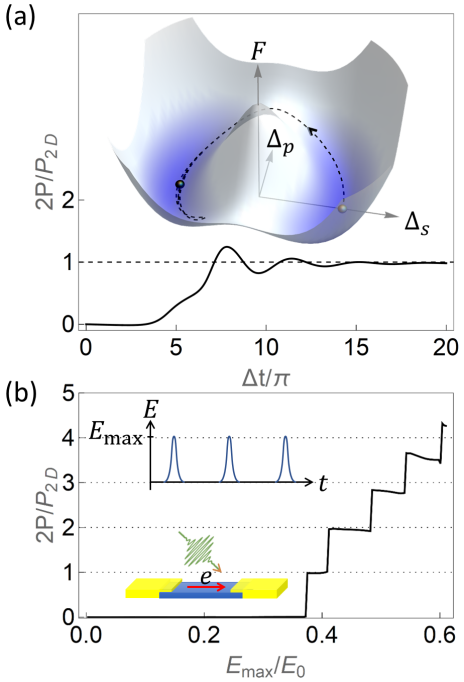

FIG. 4. Electric field pulse induced dynamics of a 2D isotropic EI. (a) The polarization as a function of time during the dynamics with P_{dis} being small. Inset is the free energy landscape $F(\Delta_s, \Delta_p)$ plotted on the $s + ip$ plane. Lower energy appears bluer. The black dashed order parameter trajectory is caused by a pulse $E(t) = E_{\max}\tanh'((t - t_0)/w)$ with maximum electric field $E_{\max} = 0.39E_0$. (b) The pumped charge by a single pulse as a function of $E_{\max}$. The units are $P_{2D} = 2k_F/\pi$ and $E_0 = \Delta^2/v_F$. Top inset is a schematic of a train of well separated pulses which can induce a 'steady' current. Bottom inset is a schematic of the device with EI shown in blue and the contacts in gold. The parameters are $g_s\nu = 0.3$, $g_p\nu = 0.58$, $\Delta = 2\Lambda e^{-1/(g_s\nu)}$, $\gamma = 0.07\Delta$ and $w = 2\pi/(2\Delta)$.

Euler-Lagrange equation $\frac{d}{dt}\frac{\delta L}{\delta \dot{\Delta}_i} = \frac{\delta L}{\delta \Delta_i}$ and is that of a point particle moving in the landscape defined by F, with kinetic energy K and driven by an electric field through L_{drive}. We find

$$L_{\text{drive}} = -P(\theta)E - s(\Delta_s, \Delta_p)E^2 + O(E^3) \tag{10}$$

where P is the adiabatic polarization in Eqs. (5) or (6), $s = \lim_{\omega\to 0}\sigma(\omega)/(2i\omega)$ and $\sigma(\omega)$ is the optical conductivity from virtual interband excitations (see [37] Sec. IV). It is natural that electric field couples linearly to the polarization and therefore provides a 'force' $E\partial_\theta P$ to rotate the order parameter in the Δ_s, Δ_p plane.

$F(\Delta_s, \Delta_p)$ gives the potential landscape in which the dynamics takes place; it has the anisotropic 'Mexican hat' form shown in Fig. 4(a). For (quasi) 1D systems in the weak coupling BCS limit [41, 42]:

$$F = -\nu\left(\Delta_s^2 + \Delta_p^2\right)\ln\frac{2\Lambda}{\sqrt{\Delta_s^2 + \Delta_p^2}} + \frac{1}{g_s}\Delta_s^2 + \frac{1}{g_p}\Delta_p^2 \tag{11}$$

where ν is density of states in the metallic phase and

$\Lambda \gg \sqrt{\Delta_s^2+\Delta_p^2}$ is a high energy cutoff [10]. The first term becomes $-\nu\int\frac{d\theta_k}{2\pi}\left(\Delta_s^2+\Delta_p^2\cos^2\theta_k\right)\ln\left(2\Lambda/\sqrt{\Delta_s^2+\Delta_p^2\cos^2\theta_k}\right)$ for a 2D isotropic Fermi surface and $\frac{d\theta_k}{2\pi}\to\frac{\sin\theta_k d\theta_k d\phi_k}{4\pi}$ for 3D where θ_k and ϕ_k are angular variables on the Fermi surface. The landscape has a local maximum at $R=0$ surrounded by a trough at $R(\theta)$ of lower values of F. The ground state minima are at $(\pm\Delta,0)$ and the pure p-wave phases at $(0,\pm\Delta_{p0})$ are saddle points with energy higher by $F_b=\nu(\Delta^2-c\Delta_{p0}^2)/2$ where c is a constant depending on the space dimension.

We may estimate the minimal electric field required to drive the system from the minimum through the p-wave saddle point by equating the potential energy barrier F_b to the work $EP(\theta=\pi/2)+\mathcal{O}(E^2)$ done by the electric field, obtaining

$$E_c\approx\kappa E_0,\quad E_0=\Delta/\xi^0=\Delta^2/v_F \tag{12}$$

where $\xi^0=v_F/\Delta$ is the coherence length (exciton size), $\kappa=\frac{1}{\pi}(1-\Delta_{p0}^2/\Delta^2)$ in 1D and $\kappa=\frac{1}{2}-\frac{1}{4}\frac{\Delta_{p0}^2}{\Delta^2}$ in 2D, and E_0 is at the order of the dielectric breakdown field. For $v_F=10^6\,\mathrm{m/s}$, $\Delta=10\,\mathrm{meV}$ and $\Delta_{p0}\ll\Delta$, such as the case of electron hole bilayers, the threshold field is $E_c\sim10^3\,\mathrm{V/cm}$ which can be easily achieved by modern optical technique. For a 100 meV gap such as that in Ta_2NiSe_5 [16, 17] (assuming it is in the BCS regime), the threshold field is about $10^5\,\mathrm{V/cm}$. At such large field, $O(E^2)$ terms in the Lagrangian will be important, which pushes the order parameter closer to zero but does not destroy the qualitative dynamics in the transient regime (See [37] Sec. IV D).

The dynamical term K has a relatively simple form if the gap never closes on the Fermi surface and the order parameter variation timescale is long compared to the inverse of the gap. For example for (quasi) 1D

$$K\approx\nu\left(\dot{R}^2/R^2+3\dot{\theta}^2\right)/12 \tag{13}$$

to lowest order in time derivatives. For higher dimensions with closed Fermi surfaces, there are $O(1)$ changes to the coefficients and, crucially, dissipation and time non-locality arises from quasiparticle excitations near the nodes of the p-wave gap when Δ_s passes zero. This dissipation also brings a correction to the pumped charge: $P\to P_{2D}+P_{\mathrm{dis}}$. To estimate P_{dis}, we observe that as the order parameter passes this gapless regime with a velocity $\dot{\Delta}_s$, the probability for exciting a particle-hole pair at k is given by the Landau-Zener formula [43]: $P_k=e^{-2\pi\delta_k^2/|\partial_t 2\Delta_s|}$ where $\delta_k=\sqrt{\xi_k^2+\Delta_p^2 f_k^2}$ is half of its minimal excitation energy during the dynamics. In 2D, summing over momenta, one obtains the number of excited quasi particles $N=\frac{k_F}{2\pi^2 v_F}|\frac{\dot{\Delta}_s}{\Delta_p}|$ and the non-adiabatic correction to the pumped charge

$$P_{\mathrm{dis}}=-P_{2D}\frac{1}{8\pi^2}\frac{|\dot{\Delta}_s|}{\Delta_p^2} \tag{14}$$

valid if $\sqrt{|\dot{\Delta}_s|}\ll|\Delta_p|$ (see [37] Sec. VI C). Therefore, if the sub-dominant p-wave coupling constant is too small such that $\Delta_{p0}\sim\Lambda e^{-\frac{1}{g\rho\nu}}<\sqrt{|\dot{\Delta}_s|/(8\pi^2)}$, this dissipative correction will dominate over the adiabatic charge.

Numerics and Experiment—We numerically solved the mean field dynamics implied by Eq. (1) for a BCS weak coupling EI in 2D, driven by a train of widely separated electric field pulses (Fig. 4(b)). Mean field dynamics [44] means that each momentum state evolves in the time dependent mean field $(\Delta_s,\Delta_p f_{k-A},\xi_{k-A})$ with $\Delta_{s,p}$ determined self consistently by the gap equation, neglecting any spatial fluctuations. We include a weak phenomenological damping γ to represent energy loss caused by, e.g., a phonon bath (see [37] Sec. VI). Each pulse drives the order parameter along the trajectory shown as the black dashed line in Fig. 4(a), advancing it by $\theta=\pi$ to stabilize the system in the other s-wave ground state. The total duration of the evolution from one minimum to the next is $T_s\approx20\pi/\Delta$ and the amount of charge pumped is $WP_{2D}/2$ where W is the width of the sample, as shown by Fig. 4(a). In a train of pulses with inter pulse separation $T_0\gg T_s$, each pulse advances the order parameter from one minimum to the next and allows it to stabilize before next pulse arrives, leading to a time-averaged current $I_0=eWk_F/(\pi T_0)$. For a $10\,\mu\mathrm{m}$ wide sample with normal state carrier density of $10^{12}\,\mathrm{cm}^{-2}$ and inter pulse time $T_0=1\,\mathrm{ns}$, the current is $I_0=255\,\mathrm{nA}$ considering spin degeneracy.

A minimum field strength $\sim E_c$ (12) is required: as the maximum electric field $E_{\max}$ of the pulse is increased beyond the threshold, the charge pumping (DC current) will onset sharply, as shown in Fig. 4(b). As $E_{\max}$ further increases, each pulse induces a rotation of more cycles which pumps more charge, giving rise to the step structure. Deviations from perfect quantization arise from fast order parameter dynamics caused by the short duration pulse. A precisely engineered long duration pulse can substantially reduce these deviations; see [37] Sec. V.

A static electric field in the DC transport regime could also drive such an order parameter rotation and charge pumping. However, unlike the case of well separated pulses, there is no time break to dump the generated heat into the environment which might destroy the system.

Discussion—We have shown theoretically that a Thouless charge pump may be realized as a collective many-body effect arising from order parameter steering in BCS type excitonic insulators. Similar dynamics and charge pumping can occur in general when the ground state order parameter and the sub dominant one have different parities under inversion. Its observation would provide both a verification of order parameter steering and a probe of the excitonic insulating state, in particular, distinguishing BCS and BEC states. It is interesting to study the dynamics in the vicinity of the BCS-BEC crossover and effects beyond mean field.

We acknowledge support from the Energy Frontier Research Center on Programmable Quantum Materials funded

by the US Department of Energy (DOE), Office of Science, Basic Energy Sciences (BES), under award No. DE-SC0019443. We thank W. Yang, D. Golez and T. Kaneko for helpful discussions.

[1] A. Kirilyuk, A. V. Kimel, and T. Rasing, Rev. Mod. Phys. **82**, 2731 (2010).
[2] J. H. Mentink, K. Balzer, and M. Eckstein, Nature Communications **6**, 6708 (2015).
[3] T. Byrnes, N. Y. Kim, and Y. Yamamoto, Nature Physics **10**, 803 (2014).
[4] J. Zhang and R. Averitt, Annu. Rev. Mater. Res. **44**, 19 (2014).
[5] D. N. Basov, R. D. Averitt, and D. Hsieh, Nature Materials **16**, 1077 (2017).
[6] D. Golež, P. Werner, and M. Eckstein, Phys. Rev. B **94**, 035121 (2016).
[7] M. Claassen, D. M. Kennes, M. Zingl, M. A. Sentef, and A. Rubio, Nature Physics **15**, 766 (2019).
[8] Z. Sun and A. J. Millis, Phys. Rev. X **10**, 021028 (2020).
[9] N. F. Mott, Philos. Mag. **6**, 287 (1961).
[10] A. Kozlov and L. Maksimov, Sov. J. Exp. Theor. Phys. **21**, 790 (1965).
[11] D. Jérome, T. M. Rice, and W. Kohn, Phys. Rev. **158**, 462 (1967).
[12] T. Portengen, T. Östreich, and L. J. Sham, Phys. Rev. B **54**, 17452 (1996).
[13] M. M. Fogler, L. V. Butov, and K. S. Novoselov, Nat. Commun. **5**, 4555 (2014).
[14] J. I. A. Li, T. Taniguchi, K. Watanabe, J. Hone, and C. R. Dean, Nature Physics **13**, 751 (2017).
[15] L. Du, X. Li, W. Lou, G. Sullivan, K. Chang, J. Kono, and R.-R. Du, Nature Communications **8**, 1971 (2017).
[16] Y. F. Lu, H. Kono, T. I. Larkin, A. W. Rost, T. Takayama, A. V. Boris, B. Keimer, and H. Takagi, Nat. Commun. **8**, 1 (2017).
[17] D. Werdehausen, T. Takayama, M. Höppner, G. Albrecht, A. W. Rost, Y. Lu, D. Manske, H. Takagi, and S. Kaiser, Science Advances **4**, eaap8652 (2018).
[18] Y. Wakisaka, T. Sudayama, K. Takubo, T. Mizokawa, M. Arita, H. Namatame, M. Taniguchi, N. Katayama, M. Nohara, and H. Takagi, Phys. Rev. Lett. **103**, 026402 (2009).
[19] T. Kaneko, T. Toriyama, T. Konishi, and Y. Ohta, Phys. Rev. B **87**, 035121 (2013).
[20] K. Sugimoto, S. Nishimoto, T. Kaneko, and Y. Ohta, Phys. Rev. Lett. **120**, 247602 (2018).
[21] G. Mazza, M. Rösner, L. Windgätter, S. Latini, H. Hübener, A. J. Millis, A. Rubio, and A. Georges, Phys. Rev. Lett. **124**, 197601 (2020).
[22] A. Kogar, M. S. Rak, S. Vig, A. A. Husain, F. Flicker, Y. I. Joe, L. Venema, G. J. MacDougall, T. C. Chiang, E. Fradkin, J. Van Wezel, and P. Abbamonte, Science **358**, 1314 (2017).
[23] H. Cercellier, C. Monney, F. Clerc, C. Battaglia, L. Despont, M. G. Garnier, H. Beck, P. Aebi, L. Patthey, H. Berger, and L. Forró, Phys. Rev. Lett. **99**, 146403 (2007).
[24] T. Kaneko, Y. Ohta, and S. Yunoki, Phys. Rev. B **97**, 155131 (2018).
[25] C. Chen, B. Singh, H. Lin, and V. M. Pereira, Phys. Rev. Lett. **121**, 226602 (2018).
[26] Y. Jia, P. Wang, C.-L. Chiu, Z. Song, G. Yu, B. Jäck, S. Lei, S. Klemenz, F. A. Cevallos, M. Onyszczak, N. Fishchenko, X. Liu, G. Farahi, F. Xie, Y. Xu, K. Watanabe, T. Taniguchi, B. A. Bernevig, R. J. Cava, L. M. Schoop, A. Yazdani, and S. Wu, "Evidence for a monolayer excitonic insulator," (2020), arXiv:2010.05390 [cond-mat.mes-hall].
[27] Y. Hu, J. W. F. Venderbos, and C. L. Kane, Phys. Rev. Lett. **121**, 126601 (2018).
[28] R. Wang, O. Erten, B. Wang, and D. Y. Xing, Nat. Commun. **10**, 1 (2019).
[29] L.-H. Hu, R.-X. Zhang, F.-C. Zhang, and C. Wu, "Interacting topological mirror excitonic insulator in one dimension," (2019), arXiv:1912.09066 [cond-mat.str-el].
[30] D. Varsano, M. Palummo, E. Molinari, and M. Rontani, Nature Nanotechnology **15**, 367 (2020).
[31] E. Perfetto and G. Stefanucci, Phys. Rev. Lett. **125**, 106401 (2020).
[32] Z. Sun and A. J. Millis, Phys. Rev. B **102**, 041110(R) (2020).
[33] D. J. Thouless, Phys. Rev. B **27**, 6083 (1983).
[34] M. J. Rice and E. J. Mele, Phys. Rev. Lett. **49**, 1455 (1982).
[35] R. D. King-Smith and D. Vanderbilt, Phys. Rev. B **47**, 1651(R) (1993).
[36] Y. Zhang, Y. Gao, and D. Xiao, Phys. Rev. B **101**, 041410(R) (2020).
[37] See Supplemental Material at [URL will be inserted by publisher] for details.
[38] Y. Murakami, D. Golež, T. Kaneko, A. Koga, A. J. Millis, and P. Werner, Phys. Rev. B **101**, 195118 (2020).
[39] R. Resta, Rev. Mod. Phys. **66**, 899 (1994).
[40] J. Goldstone and F. Wilczek, Phys. Rev. Lett. **47**, 986 (1981).
[41] A. Altland and B. D. Simons, *Condensed Matter Field Theory* (Cambridge University Press, Cambridge, 2010).
[42] Z. Sun, M. M. Fogler, D. N. Basov, and A. J. Millis, Phys. Rev. Research **2**, 023413 (2020).
[43] C. Wittig, J. Phys. Chem. B **109**, 8428 (2005).
[44] R. A. Barankov, L. S. Levitov, and B. Z. Spivak, Phys. Rev. Lett. **93**, 160401 (2004).